

Beyond Fully Supervised Pixel Annotations: Scribble-Driven Weakly-Supervised Framework for Image Manipulation Localization

Songlin Li[†], Guofeng Yu[†], Zhiqing Guo^{*}, Yunfeng Diao, Dan Ma, Gaobo Yang, and Liejun Wang

Abstract—Deep learning-based image manipulation localization (IML) methods have achieved remarkable performance in recent years, but typically rely on large-scale pixel-level annotated datasets. To address the challenge of acquiring high-quality annotations, some recent weakly supervised methods utilize image-level labels to segment manipulated regions. However, the performance is still limited due to insufficient supervision signals. In this study, we explore a form of weak supervision that improves the annotation efficiency and detection performance, namely scribble annotation supervision. We re-annotated mainstream IML datasets with scribble labels and propose the first scribble-based IML (Sc-IML) dataset. Additionally, we propose the first scribble-based weakly supervised IML framework. Specifically, we employ self-supervised training with a structural consistency loss to encourage the model to produce consistent predictions under multi-scale and augmented inputs. In addition, we propose a prior-aware feature modulation module (PFMM) that adaptively integrates prior information from both manipulated and authentic regions for dynamic feature adjustment, further enhancing feature discriminability and prediction consistency in complex scenes. We also propose a gated adaptive fusion module (GAFM) that utilizes gating mechanisms to regulate information flow during feature fusion, guiding the model toward emphasizing potential tampered regions. Finally, we propose a confidence-aware entropy minimization loss (\mathcal{L}_{CEM}). This loss dynamically regularizes predictions in weakly annotated or unlabeled regions based on model uncertainty, effectively suppressing unreliable predictions. Experimental results show that our method outperforms existing fully supervised approaches in terms of average performance both in-distribution and out-of-distribution. Our code is available on <https://github.com/vpsg-research/SCAF>.

Index Terms—Image manipulation localization, weakly supervised, scribble, consistency, uncertainty.

I. INTRODUCTION

This work was supported in part by the National Natural Science Foundation of China under Grant 62302427 and Grant 62462060, in part by the Natural Science Foundation of Xinjiang Uygur Autonomous Region under Grant 2023D01C175, in part by the TianshanTalent Training Program under Grant 2022TSYCLJ0036.

*Corresponding author, [†]Equal contribution.

Songlin Li, Guofeng Yu, Zhiqing Guo, Dan Ma, and Liejun Wang are with the School of Computer Science and Technology, Xinjiang University, Urumqi 830046, China. (e-mail: lisl@stu.xju.edu.cn; yuguofeng@stu.xju.edu.cn; guozhiqing@xju.edu.cn; madan@xju.edu.cn; wljxju@xju.edu.cn).

Gaobo Yang is with the College of Computer Science and Electronic Engineering, Hunan University, Changsha 410082, China (email: yang-gaobo@hnu.edu.cn).

Yunfeng Diao is with the School of Computer Science and Information Engineering, Hefei University of Technology, Hefei, China. (email: diaoyunfeng@hfut.edu.cn).



Scribble annotations mark only the main structure of objects (blue for authentic, red for manipulated) and are 69 times faster to produce than pixel-level annotations.

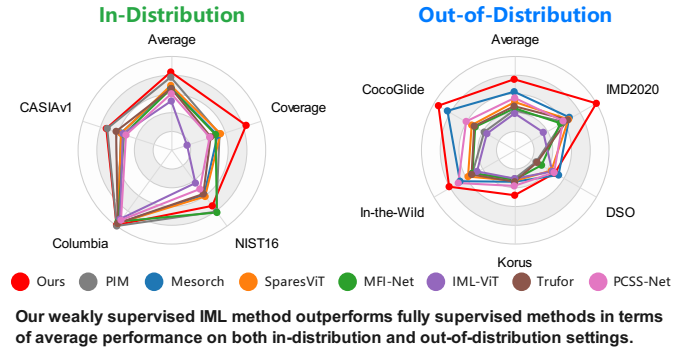


Fig. 1. Compared with the existing IML methods in labeling efficiency and performance.

MALICIOUS manipulated images will spread false information and seriously endanger social harmony. Thus, image manipulation localization (IML) technology, which aims at accurately segmenting the manipulated region, has been widely studied.

In recent years, deep learning techniques have significantly advanced the performance of IML methods, particularly when supported by large-scale pixel-level annotated datasets. Fully supervised approaches can leverage dense pixel annotations to learn fine-grained manipulation features, achieving state-of-the-art localization results on various benchmark datasets. However, acquiring high-quality pixel-level annotations is both time-consuming and labor-intensive, which greatly limits the scalability and practical application of these methods. In real-world scenarios, obtaining large-scale high-precision pixel annotations is often infeasible, especially as data diversity and scale continue to expand. To reduce annotation costs, weakly supervised IML methods have emerged in recent years, typically relying on image-level labels to guide the localization of manipulated regions. While such methods alleviate the dependence on dense annotations, their limited supervision signals lead to clear bottlenecks in localization accuracy

and generalization capability. A substantial performance gap still exists between weakly supervised and fully supervised approaches.

To address these challenges, this paper explores a form of weak supervision, namely scribble annotations, which takes into account the efficiency of labeling and the amount of supervision information, as shown in Fig. 1. Scribble annotations enable rapid labeling of large-scale IML datasets while providing informative cues for localization tasks. We re-annotated several mainstream IML datasets, including 5,123 images from CASIAv2 [1], 70 images from Coverage [2], 130 images from Columbia [3], and 414 images from NIST16 [4], resulting in a total of 5,737 images. This constitutes the first scribble-based IML (Sc-IML) dataset. During annotation, annotators used CVAT¹ to draw scribbles on the manipulated regions based on their first impression, without referring to the ground truth. To ensure high-quality data, the annotation process was cross-verified by three reviewers. Each image took approximately 20 seconds to annotate. However, existing studies have not reported the time required to manually annotate a pixel-level mask for a manipulated image. To address this issue, we organized 10 experienced computer vision researchers to follow the same annotation process as the scribble annotations. Each researcher randomly selected 10 images from the CASIAv2 dataset for pixel-level annotation, with an average annotation time of approximately 23 minutes per image. This shows that scribble annotation is 69 times faster than pixel-level annotation. Although scribble annotations are significantly more efficient and convenient compared to pixel-level masks, they still face two major limitations: (1) Scribble annotation is a highly subjective form of weak supervision. Different annotators may have varying interpretations of the manipulated regions, boundaries, and details, resulting in significant inconsistency among the scribble annotations. (2) Scribble labels offer limited pixel-level supervision, causing the model to lack confidence in classifying unmarked regions and leading to prediction uncertainty.

Based on this, we propose the first weakly supervised IML framework utilizing scribble annotations, namely SCAF. To address the challenges of prediction inconsistency and uncertainty under scribble-based weak supervision in IML datasets, we introduce a series of innovative strategies. To resolve inconsistency, we employ self-supervised training with a structural consistency loss, which constrains the model to produce consistent predictions under multi-scale and augmented inputs. We also propose a prior-aware feature modulation module (PFMM) that adaptively integrates prior information from both manipulated and authentic regions for dynamic feature adjustment, and incorporate coordinate attention to efficiently model spatial dependencies, thereby significantly enhancing the discriminability and scene adaptability of feature representations. To tackle prediction uncertainty, we propose a gated adaptive fusion module (GAFM) that regulates information flow through multi-branch channel splitting and adaptive dynamic fusion. This module not only highlights critical features and suppresses redundancy, but also leverages

scribble supervision to guide the model’s attention toward potential manipulated regions. Additionally, we propose a confidence-aware entropy minimization loss (\mathcal{L}_{CEM}), which dynamically filters model outputs based on uncertainty and applies adaptive entropy regularization to weakly annotated or unlabeled regions. This effectively suppresses unreliable predictions and improves model confidence and generalization in key areas.

In summary, our contributions to IML are as follows:

- We propose the Sc-IML, the first scribble annotated dataset specifically designed for weakly supervised IML. Sc-IML effectively bridges the gap between costly pixel-level annotations and coarse image-level supervision by providing valuable spatial cues for the development and evaluation of weakly supervised IML methods, thereby advancing research in this field.
- We propose the first weakly supervised IML framework based on scribble annotations, which outperforms existing fully supervised methods in terms of both in-distribution and out-of-distribution average performance.
- We propose a PFMM that adaptively integrates prior information from both manipulated and authentic regions to achieve dynamic feature modulation. By further incorporating coordinate attention to efficiently model spatial dependencies, thereby significantly enhancing feature discrimination and scene adaptability.
- We propose a GAFM that regulates information flow through multi-branch channel splitting and adaptive dynamic fusion. This module not only highlights critical features and suppresses redundancy, but also leverages scribble annotations to guide the model’s attention toward potential manipulated regions.
- We propose a confidence-aware entropy minimization loss, which adaptively regularizes predictions in weakly annotated or unlabeled regions, significantly suppresses unreliable predictions, and enhances model confidence and generalization in critical areas.

II. RELATED WORK

A. Fully Supervised Image Manipulation Localization

With the continuous development of deep learning and the emergence of large-scale datasets, fully supervised IML methods have achieved remarkable results. For example, Guillaro et al. [5] proposed an IML framework that combines RGB data with noise-resistant fingerprints for IML. Chen et al. [6] effectively enhanced the detection of boundary artifacts in IML by refining edge features and leveraging multi-feature fusion. Kong et al. [7] leveraged pixel inconsistency to model global and local dependencies, enabling generalizable localization across various manipulation types.

B. Weakly Supervised Image Manipulation Localization

To reduce annotation costs, weakly supervised IML methods have been developed to segment manipulated regions using only image-level labels. For example, Zhai et al. [8] introduced a self-consistency learning approach with image-level labels

¹<https://app.cvat.ai/>

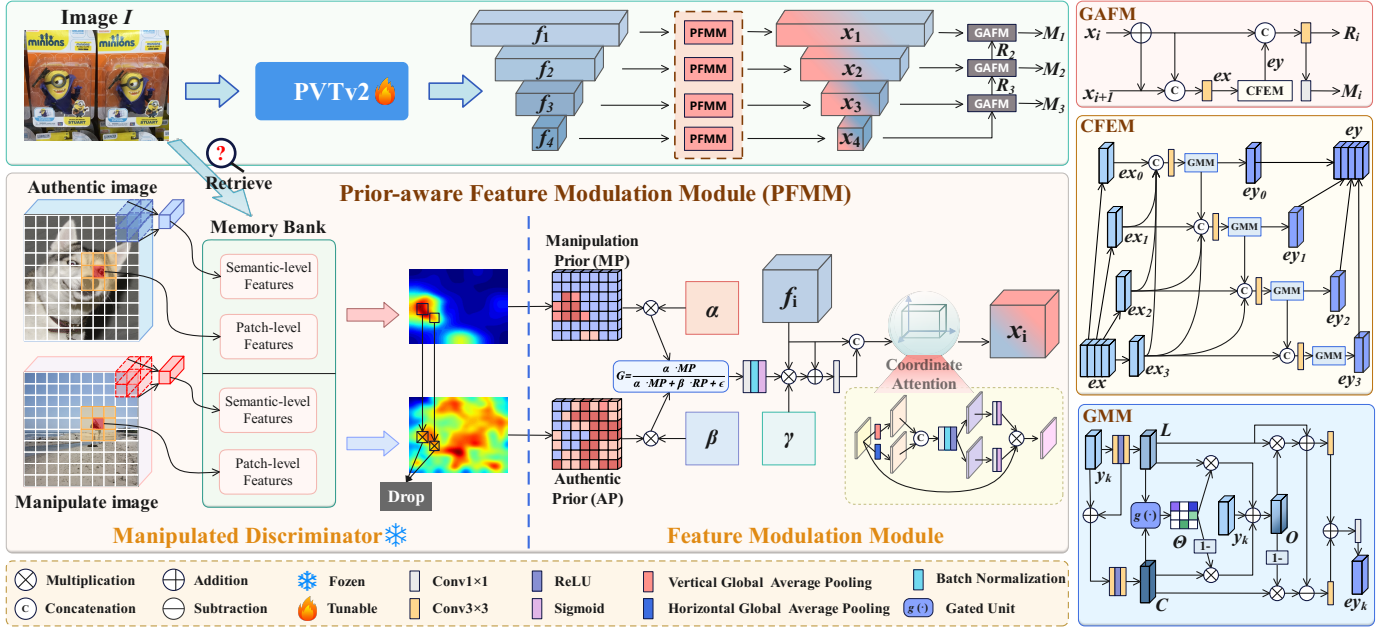


Fig. 2. The overall architecture of the proposed SCAF. The model comprises two key modules: the prior-aware feature modulation module (PFMM) and the gated adaptive fusion module (GAFM). It is worth noting that the PFMM consists of a manipulated discriminator (MD) and a feature modulation module (FMM).

and multi-source consistency for improved IML. Zhou et al. [9] proposed a self-optimization framework that iteratively refines pseudolabels to enhance boundary accuracy. Li et al. [10] designed a cross-contrastive learning network that utilizes image-level labels and multi-stream feature fusion for IML. Bai [11] proposed a WSCCL that uses point correspondences to detect and localize manipulated regions. Notably, these are the only published studies on weakly supervised IML to date.

Although fully supervised methods achieve high localization accuracy, they rely on large-scale high-quality pixel-level annotations, which are costly and time-consuming to obtain. Their scalability is further limited by the lack of such data in real-world scenarios. Weakly-supervised IML methods using image-level labels greatly reduce annotation costs but lack spatial cues, making precise localization difficult and often missing subtle manipulations. To address these challenges, we propose a novel weakly supervised IML approach with scribble annotations. Scribbles provide crucial spatial information to the model, guiding it to learn the spatial distribution of manipulated regions while significantly improving annotation efficiency. Our method outperforms existing fully supervised methods in terms of average performance, both in-distribution and out-of-distribution.

III. METHODOLOGY

A. Overview

The overall architecture of SCAF, is shown in Fig. 2. Specifically, the input image I is first processed by PVTv2 [12] to extract multi-scale features f_i , and these features are then modulated in the prior-aware feature modulation module (PFMM) using the prior to integrate them into x_i . Finally, the features are fused by the gated adaptive fusion module

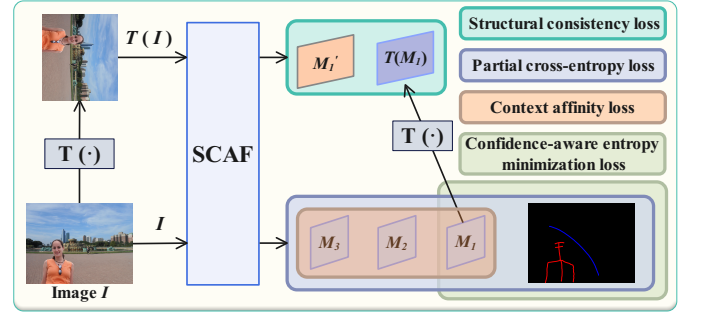


Fig. 3. The training process of the proposed model. $T(\cdot)$ denotes random rotations, scaling, and flipping.

(GAFM) to produce the final predicted mask. The training process of the model is illustrated in Fig. 3. An image I is input into the SCAF to generate the primary output M_1 as well as auxiliary outputs M_2 and M_3 . Additionally, a randomly transformed version of I , denoted as $T(I)$ (which may include rotations, scaling, or flipping), is also fed into the SCAF to obtain M_1' , which, together with M_1 , is used to compute the structural consistency loss (\mathcal{L}_{SC}) [13]. Furthermore, M_1 is jointly supervised by the partial cross-entropy loss (\mathcal{L}_{PCE}), context affinity loss (\mathcal{L}_{CA}) [14], and confidence-aware entropy minimization loss (\mathcal{L}_{CEM}), while M_2 and M_3 are optimized using only \mathcal{L}_{CA} and \mathcal{L}_{PCE} .

B. Prior-aware Feature Modulation Module

For scribble annotations, annotators typically mark the tampered regions in an image by freely drawing rough scribbles. Since this annotation method heavily relies on personal subjective judgment, different annotators may have varying understandings of the tampered regions, interpretations of

boundaries, and levels of attention to detail. Even for the same image, the content of the scribble annotations can differ significantly. This subjectivity and randomness lead to considerable label inconsistency within the training set, which in turn affects the model’s ability to accurately identify tampered regions and generalize to new data. In complex scenarios, this often results in unstable and unreliable predictions. To address the inconsistency caused by subjective scribble annotations, we propose a prior-aware feature modulation module (PFMM). As shown in the lower left of Fig. 2, PFMM is composed of two parts: the manipulated discriminator (MD) and the feature modulation module (FMM). The core idea is to utilize manipulated priors (MP) and authentic prior (AP) generated by the MD, and then leverage these priors within the FMM to dynamically modulate the features f_i in a targeted manner. By explicitly introducing prior knowledge, PFMM can effectively mitigate the noise and bias introduced by subjective scribble annotations, guiding the model to focus on more objective region distributions. This mechanism enhances the model’s discriminability for manipulated regions and improves prediction consistency and robustness.

1) Manipulated discriminator (MD): Existing research [15] has demonstrated that patch-level features are effective for detecting subtle anomalies. However, they lack explicit suppression of semantic bias, which becomes particularly evident in cross-domain scenarios. To address this limitation, we propose a selective suppression mechanism based on semantic-level features, which builds upon patch-level representations. By memorizing multi-scale semantics from both authentic and manipulated images, our method adaptively suppresses features that are highly similar to those stored in the memory bank during inference. This enables the generation of precise authentic region priors and manipulated region priors. Specifically, taking the training process of authentic images as an example, we first extract multi-layer features using the PVTv2. Each layer’s feature map is then partitioned into overlapping patches with a stride of 1, resulting in a set of local patch features p_j^s . To further incorporate local contextual information, we perform weighted fusion of each patch and its eight spatial neighbors to obtain \tilde{p}_j^s , as formulated below:

$$\tilde{p}_j^s = \sum_{n \in \mathcal{N}(j)} w_n p_n^s \quad (1)$$

where $\mathcal{N}(j)$ denotes the 3×3 neighborhood centered at j , and w_j represents the weighting coefficient. The collection of \tilde{p}_j^s constitutes the patch-level feature P_s for an image. We store the patch-level features P_s of all images in the training set to construct a patch-level memory bank \mathcal{B}_p :

$$\begin{cases} P_s = \{\tilde{p}_j^s \mid j = 1, \dots, T\} \\ \mathcal{B}_p = \{P_s \mid s = 1, \dots, N\} \end{cases} \quad (2)$$

where T denotes the total number of local patch features in a sample. N denotes the number of training samples. For the construction of the semantic-level memory bank \mathcal{B}_s , we first extract features from the authentic training samples using the backbone network, and reduce the channel dimension of the extracted features to 256 to obtain the feature set $\{v_m\}_{m=1}^N$.

These features are then subjected to L2 normalization. Finally, the semantic features of all training images are stored to form the memory bank:

$$\begin{cases} \tilde{v}_m = v_m / \|v_m\|_2 \\ \mathcal{B}_s = \{\tilde{v}_m \mid m = 1, \dots, N\} \end{cases} \quad (3)$$

The model constructs a memory bank of authentic region features by learning from a large number of real images. However, this bank is filled with highly similar features, resulting in redundancy and bias, which leads the model to overgeneralize dominant authentic region features. During inference, this mechanism causes subtle manipulated features to be easily overwhelmed by the abundance of highly matching authentic features, thereby reducing the saliency of tampered regions and ultimately lowering localization accuracy. To address this issue, we actively identify and suppress redundant authentic feature noise, which relatively amplifies and highlights manipulated features that represent inconsistencies. In this way, the model shifts from passively learning authentic image features to actively capturing the distinctive traces of manipulation. The details are as follows:

$$q_{sup} = \left(1 - \max_m \left(\frac{q \times v_m}{\|q\|_2 \|v_m\|_2} \right)\right) \times q \quad (4)$$

where q denotes the current input feature, which is compared with each feature v_m in \mathcal{B}_s to compute the maximum cosine similarity. This process suppresses regions that are overly similar to authentic features from the training set and highlights manipulated features, resulting in q_{sup} . Finally, the Euclidean distance between q_{sup} and its nearest feature P_s in \mathcal{B}_p is calculated. It can be formulated as follows:

$$\text{Score}(q_{sup}) = \|q_{sup} - P_s\|_2 \quad (5)$$

By scoring each location in the input image, we obtain a prior map of manipulated regions. Similarly, training on manipulated images yields a prior map for authentic regions. However, since manipulated images contain both authentic and manipulated areas, the authentic prior may include false activations. To address this, we compute the cosine similarity between the manipulated and authentic priors, removing falsely activated regions to obtain a purified authentic prior.

2) Feature modulation module (FMM): FFM is designed to adaptively modulate the feature f_i using prior information, thereby alleviating the adverse effects caused by the inconsistency of scribble annotations. Specifically, FFM utilizes learnable manipulated region weight α and authentic region weight β to perform weighted normalization of the prior knowledge, resulting in the computation of the manipulated region probability response G , as formulated below:

$$G = \frac{\alpha \times MP}{\alpha \times MP + \beta \times AP + \epsilon} \quad (6)$$

where ϵ is a small constant added to prevent division by zero. This controllable probabilistic modeling approach allows the module to adaptively adjust its sensitivity to different regions based on the data distribution, effectively reducing the impact of label inconsistency or prior noise on performance. Then, G is passed through a 1×1 convolution, batch normalization, and

a Sigmoid activation function to generate an enhanced feature map G_e for each spatial location. This is further regularized residually by a learnable parameter γ to obtain the feature F , as follows:

$$F = \text{Conv1}(f_i + \gamma \times G_e \times f_i) \quad (7)$$

where Conv1 denotes a 1×1 convolution. Finally, coordinate attention is applied to the concatenated features of F and f_i , resulting in the output feature x_i . Coordinate attention captures both spatial location information and channel inter-dependencies, further enhancing the model's ability to localize and discriminate manipulated regions.

In summary, PFMM explicitly incorporates manipulated and authentic priors to effectively alleviate the adverse effects of inconsistency and label noise introduced by scribble annotations. By leveraging prior-guided feature modulation, the model is able to focus on more objective and reliable regional cues, thereby enhancing both the accuracy and generalization ability of tampering localization.

C. Gated Adaptive Fusion Module

In scribble-based weakly supervised IML, annotations are sparse and irregular, making it challenging for models to fully localize manipulated regions. This incomplete supervision introduces significant uncertainty during training and hampers the detection of subtle manipulations, often leading to missed or false detections. Furthermore, manipulated regions can exhibit diverse spatial distributions and weak visual clues, which are hard to capture using conventional feature aggregation or single-scale modeling. To address these issues, we propose a gated adaptive fusion module (GAFM), as shown on the right side of Fig. 2, which consists of a core channel-aware feature enhancement module (CFEM) and a gated modulation module (GMM). The GAFM aggregates multi-scale contextual features and employs both the CFEM and GMM to group channels and progressively perform gated fusion, thereby adaptively suppressing feature uncertainty and enhancing the richness and discriminability of the feature representations. Specifically, the fused feature e_x , obtained by merging x_i and x_{i+1} , is first input into CFEM, where it is evenly split into four groups along the channel dimension.

$$e_x = [ex_0, ex_1, ex_2, ex_3], \quad ex_k \in \mathbb{R}^{B \times \frac{C}{4} \times H \times W} \quad (8)$$

Then, each group feature ex_j is concatenated with its neighboring groups or the output of the previous GMM, and sequentially passed through a 3×3 convolution and the GMM, forming a progressive information fusion flow.

$$\begin{cases} y_k = \text{Conv3}(\text{Cat}(\text{Cat}_{|z=k}^3 ex_z, \mathbb{I}(k > 0) \times ey_{k-1})) \\ ey_k = \text{GMM}(y_k) \end{cases} \quad (9)$$

where Conv3 denotes a 3×3 convolution. $\text{Cat}_{|z=k}^3$ denotes the concatenation of all ex_n for $n = j$ to 3 in sequence. $\mathbb{I}(k > 0)$ denotes the indicator function, which returns 1 if $k > 0$, and 0 otherwise. The GMM employs a gating mechanism to achieve adaptive recalibration and interaction between local and global features, thereby enhancing the modeling capability for fine-grained representations. Specifically, the feature y_k

is first processed through two separate sequences of 3×3 convolutional layers followed by ReLU activations, resulting in two distinct feature branches.

$$\begin{cases} L = \text{Conv3}(\text{ReLU}(\text{Conv3}(y_k))) \\ C = \text{Conv3}(\text{ReLU}(\text{Conv3}(L + y_k))) \end{cases} \quad (10)$$

Subsequently, the extracted local-detail feature L and contextual semantic feature C are concatenated along the channel dimension and fed into a gating unit $g(\cdot)$ [16]. By effectively leveraging the complementary relationship between these two types of features, the gating unit adaptively generates a more accurate gating coefficient α , enabling precise modulation and enhancement of features of the manipulated region. It can be formulated as:

$$\begin{cases} \theta = g(\text{Cat}(L, C)) \\ O = y_j + \theta \times L + (1 - \theta) \times C \end{cases} \quad (11)$$

Due to the limited pixel-level supervision provided by scribble-based annotations, the model may confuse features of manipulated regions with those of the authentic background, leading to ambiguous localization. To address this, we construct a complementary reverse mask $(1 - O)$ from the feature map O and combine it with feature C to obtain the authentic background features. We enhance the manipulated region's feature representation O with feature L and applying a residual connection. Subsequently, the difference between the manipulated-enhanced feature Me and the authentic background features is computed to highlight subtle or latent anomalies within the manipulated regions, resulting in the differential feature D . Then, the manipulated-enhanced feature Me is fused with the differential feature D to obtain the output feature ey_j , which can be expressed as $ey_k = \text{Conv1}(Me + D)$.

The GMM enables the model to adaptively focus on manipulated regions, enhancing manipulated features while suppressing background features. Finally, we concatenate the outputs from multiple stages of the GMM to obtain the feature ey , which can be expressed as $ey = \text{Cat}_{|k=0}^3 ey_k$.

Since each stage of the GMM focuses on adaptive modeling of specific sub-channel features, these features are inherently complementary. By concatenating them along the channel dimension, the model maximally preserves the heterogeneous information across groups, thereby providing richer contextual cues for subsequent integration and enhancing the perception and representation of complex manipulated regions.

D. Confidence-aware Entropy Minimization Loss

In scribble-based weakly supervised IML, the sparsity of supervision signals makes it difficult to adequately constrain the model's learning. While entropy minimization is an effective strategy for leveraging unlabeled regions, blindly applying it may cause the model to become "over-confident" on unreliable predictions, amplifying errors and resulting in unstable training. To address this issue, we propose a confidence-aware entropy minimization loss (\mathcal{L}_{CEM}). This loss applies entropy minimization only to unlabeled pixels whose current predictions are deemed reliable based on a confidence threshold. Additionally, a weak regularization term is applied to the

TABLE I

THE DATASET USED IN OUR EXPERIMENTS. COPY-MOVE, SPLICING, AND INPAINTING ARE ABBREVIATED AS CM, SP, AND IP, RESPECTIVELY.

Dataset	Nums	#CM	#SP	#IP	Train	Test
CASIAv2	5123	3295	1828	0	5123	0
CASIAv1	920	459	461	0	0	920
Coverage	100	100	0	0	70	30
Columbia	180	0	180	0	130	50
NIST16	564	68	288	208	414	150
CocoGlide	512	-	-	-	0	512
In-the-wild	201	0	201	0	0	201
Korus	220	-	-	-	0	220
DSO	100	0	100	0	0	100
IMD2020	2010	-	-	-	0	2010

annotated regions to directly encourage the model to produce predictions with higher confidence and sharper boundaries. Specifically, the model primary outputs $\mathbf{M}_1 \in \mathbb{R}^{B \times 1 \times H \times W}$, where each pixel produces a probability value $\mathbf{m}_t \in [0, 1]$. The Shannon entropy $\mathcal{H}(\cdot)$ for each pixel is defined as follows:

$$\mathcal{H}(\mathbf{m}_t) = -[\mathbf{m}_t \log \mathbf{m}_t + (1 - \mathbf{m}_t) \log (1 - \mathbf{m}_t)] \quad (12)$$

To avoid introducing noise from regions where the model's predictions are unreliable, we perform entropy minimization only on unlabeled pixels where the model already exhibits high confidence. The loss \mathcal{L}_{un} is defined as the average entropy over unlabeled pixels whose predicted entropy is below a threshold of 0.5:

$$\mathcal{L}_{un} = \frac{\sum_{t \in \mathcal{U}} \mathcal{H}(\mathbf{m}_t) \cdot \mathbb{I}(\mathcal{H}(\mathbf{m}_t) < 0.5)}{\sum_{t \in \mathcal{U}} \mathbb{I}(\mathcal{H}(\mathbf{m}_t) < 0.5) + \epsilon} \quad (13)$$

where \mathcal{U} denotes the set of unlabeled pixels. Meanwhile, we also compute the average entropy over labeled pixels as a weak regularization penalty, encouraging the model to make confident predictions in known regions. This loss, denoted as \mathcal{L}_{la} , is defined as follows:

$$\mathcal{L}_{la} = w_{weak} \cdot \frac{\sum_{t \in \mathcal{G}} \mathcal{H}(\mathbf{m}_t)}{|\mathcal{G}| + \epsilon} \quad (14)$$

where \mathcal{G} denotes the set of labeled pixels and $|\mathcal{G}|$ is the total number of labeled pixels. The final mixed entropy loss \mathcal{L}_{ent} is defined as the sum of \mathcal{L}_{un} and \mathcal{L}_{la} . To ensure stable training, we adopt a weight ramp-up strategy, introducing a dynamic weight $\lambda(T)$ to modulate \mathcal{L}_{ent} .

$$\lambda(T) = w_{max} \cdot \exp \left(- \left(1 - \frac{\min(T, ramp)}{ramp} \right)^2 \right) \quad (15)$$

where T denotes the current epoch and $ramp$ represents the ramp-up period. During this period, $\lambda(T)$ increases smoothly from 0 to its maximum value w_{max} . In this work, we set w_{max} and w_{weak} to 0.1, which is chosen to balance training stability and final model performance. Thus, the final loss term is defined as $\mathcal{L}_{CEM} = \lambda(T) \cdot \mathcal{L}_{ent}$.

IV. EXPERIMENTS AND RESULTS

A. Datasets

Our experiments primarily utilize 9 mainstream benchmark datasets: NIST16 [4], CASIA [1], Columbia [3], Coverage [2],

TABLE II

COMPARISON WITH OTHER ADVANCED WEAKLY SUPERVISED IML METHODS.

Method	Pub.	CASIAv1.0	Coverage	NIST16	IMD2020	Columbia
WSCL	ICCV'23	0.153	0.201	0.099	0.173	0.362
EdgeCAM	ESWA'24	0.301	0.262	0.254	0.242	0.470
SOWCL	ICASSP'25	0.334	0.239	0.288	0.259	0.385
WSCCL	KBS'25	0.349	0.281	0.278	0.259	0.516
Ours	-	0.716	0.827	0.721	0.580	0.979

IMD2020 [17], CocoGlide [18], In-the-Wild [19], DSO [20], Korus [21]. The dataset partitioning is presented in Table I.

B. Implementation Details

In this study, we used PVTv2 [12] pre-trained on ImageNet as the backbone. During training, all images were resized to 512×512 . The model was trained with a batch size of 32 using the AdamW optimizer. The initial learning rate was set to $1e-4$ and decayed by a factor of 0.1 every 50 epochs. Training was performed on 4 NVIDIA 4090 GPUs, with a total of 70 epochs.

C. Comparison with SOTA Methods

Pixel-level F1 and AUC are standard metrics for IML, but recent research [22] show that pixel-level AUC exhibits overconfidence in IML. Therefore, we evaluate all experiments using the F1-score with a fixed threshold of 0.5.

Image manipulate localization. As shown in Table II, we compare our method with existing weakly supervised IML approaches, including WSCL [8], EdgeCAM [9], SOWCL [10], and WSCCL [11]. While these methods use image-level labels as supervision, our method leverages scribble annotations. The results clearly demonstrate that our approach outperforms all competitors across all datasets, indicating that scribble-based supervision significantly improves manipulation localization performance. The spatial information provided by scribble annotations offers more effective constraints, leading to more accurate detection and localization of tampered regions. Table III presents a comparison with several state-of-the-art fully supervised methods, such as MVSS-Net [23], PCSS-Net [24], Trufor [5], MFI-Net [25], SparseViT [26], PIM [27], and Mesorch [28], evaluated under both in-distribution and out-of-distribution settings. Our weakly supervised method not only achieves higher average performance than fully supervised baselines under standard conditions, but also demonstrates stronger generalization to previously unseen manipulation scenarios. This enhanced generalization is attributed to the balance between annotation efficiency and effective supervision achieved by scribble annotations, which provide direct spatial guidance with minimal labeling effort and help prevent overfitting to dense pixel-level labels. It is worth noting that all fully supervised methods were retrained on the same benchmarks as ours for a fair comparison. However, since among the weakly supervised methods only WSCL has publicly available code, we retrained only WSCL, while the results for the other methods are taken directly from their published papers.

Visual comparison. Fig. 4 presents segmentation results of our proposed model and several SOTA fully supervised

TABLE III
COMPARISON WITH OTHER ADVANCED FULLY SUPERVISED IML METHODS.

Method	Pub.	In-Distribution					Out-of-Distribution					
		NIST16	CASIAv1.0	Columbia	Coverage	Average	CocoGlide	In-the-Wild	Korus	DSO	IMD2020	Average
MVSS-Net	ICCV'21	0.428	0.385	0.835	0.344	0.498	0.319	0.277	0.098	0.241	0.249	0.237
PCSS-Net	TCSVT'22	0.509	0.503	0.905	0.424	0.585	0.344	0.407	0.229	0.284	0.350	0.323
Trufor	CVPR'23	0.584	0.603	0.953	0.435	0.644	0.287	0.310	0.200	0.165	0.375	0.267
IML-ViT	AAAI'24	0.440	0.529	0.906	0.168	0.511	0.200	0.270	0.181	0.272	0.209	0.226
MFI-Net	TSCVT'24	0.817	0.524	0.938	0.497	0.644	0.283	0.300	0.186	0.194	0.329	0.258
SparesViT	AAAI'25	0.616	0.557	0.958	0.546	0.669	0.311	0.333	0.193	0.268	0.381	0.297
PIM	TPAMI'25	0.587	0.548	0.954	0.504	0.648	0.481	0.392	0.203	0.316	0.395	0.357
Mesorch	AAAI'25	0.802	0.703	0.981	0.531	0.754	0.218	0.299	0.182	0.160	0.346	0.241
Ours	-	0.721	0.716	0.979	0.827	0.811	0.546	0.467	0.282	0.290	0.580	0.433

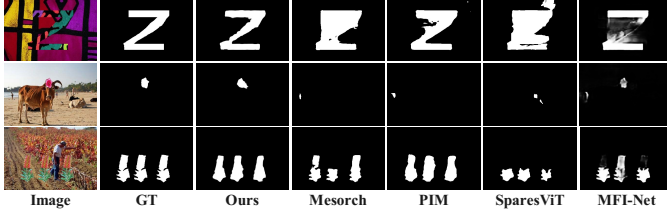


Fig. 4. Visualization results of different methods.

TABLE IV
ABLATION STUDY RESULTS OF MODEL COMPONENTS.

Method	NIST16	CASIAv1.0	Columbia	Coverage	Average
(a) B	0.404	0.396	0.841	0.621	0.566
(b) B+GAFM	0.668	0.540	0.960	0.618	0.697
(d) Ours	0.721	0.716	0.979	0.827	0.811

TABLE V
THE ABLATION STUDY FOR OUR LOSS FUNCTIONS.

\mathcal{L}_{PCE}	\mathcal{L}_{CA}	\mathcal{L}_{SC}	\mathcal{L}_{CEM}	NIST16	CASIAv1.0	Columbia	Coverage
✓				0.308	0.603	0.900	0.698
✓	✓			0.642	0.654	0.933	0.694
✓	✓	✓		0.618	0.707	0.962	0.732
✓	✓	✓	✓	0.721	0.716	0.979	0.827

methods under challenging scenarios, including large-scale manipulations, small-scale manipulations, and multi-object manipulations. Clearly, our weakly supervised approach significantly outperforms other baseline methods in terms of localization performance. Specifically, our model accurately identifies the large manipulated regions in the first row, yielding clear and complete segmentations with well-defined boundaries, while the comparison methods often suffer from false positives. In the second row, featuring small-scale manipulations, our method continues to deliver precise localization, whereas the other methods almost entirely fail. For the multi-object manipulations in the third row, our approach provides accurate segmentation of all manipulated objects. Although PIM also produces relatively complete results in this scenario, our method demonstrates superior performance in capturing fine details.

D. Ablation Study

As shown in Table IV, introducing the GAFM significantly improves performance compared to the baseline model, underscoring the importance of adaptive information regulation in

TABLE VI
ROBUSTNESS EXPERIMENTS ON ONLINE SOCIAL NETWORKS.

Method	App				
	None	Facebook	WeiBo	WeChat	WhatsApp
MFI-Net	0.524	0.449	0.455	0.363	0.474
SparesViT	0.557	0.493	0.529	0.365	0.506
PIM	0.548	0.581	0.566	0.505	0.585
Mesorch	0.703	0.671	0.655	0.583	0.677
Ours	0.716	0.685	0.690	0.623	0.686

TABLE VII
COMPARISON OF MODEL PARAMETERS AND COMPUTATIONAL COMPLEXITY.

Metrics	MFI-Net	SparesViT	PIM	Mesorch	Ours
Params (M)	32.54	50.22	152.47	84.96	27.57
Flops (G)	36.25	41.46	682.88	145.93	35.39

feature fusion. When all modules are integrated, our complete model achieves the highest F1-scores across all benchmark datasets, highlighting the synergistic effect of the proposed structural designs and feature modulation strategies. Table V further analyzes the contributions of each loss function. Using only \mathcal{L}_{PCE} results in limited performance gains. The addition of \mathcal{L}_{SC} and \mathcal{L}_{CA} consistently enhances performance, reflecting the advantages of enforcing structural invariance and context-aware modeling. Notably, incorporating the \mathcal{L}_{CEM} yields the most significant improvement. This shows the effectiveness of dynamically regularizing predictions in weakly annotated or unlabeled regions, thereby enhancing model robustness and generalization.

E. Robustness and Efficiency of the Model

With the rapid development of the internet, online social platforms have become a primary channel for image dissemination. To evaluate the robustness of our model under such conditions, we followed the same benchmark as [29] and applied compression through platforms such as Facebook, Weibo, WeChat, and WhatsApp. As shown in Table VI, our model consistently maintains significant performance advantages after online transmission. Furthermore, as illustrated in Table VII, our model not only demonstrates outstanding performance but also features the fewest parameters and the lowest computational complexity.

V. CONCLUSION

In this work, we present and release the first scribble-annotated IML dataset, Sc-IML, filling an important gap in weakly supervised annotation resources for the field. We also propose the first scribble-based weakly supervised IML framework, which incorporates structural consistency, prior-aware feature modulation, and gated adaptive fusion modules, significantly boosting model robustness and detection accuracy. Furthermore, the confidence-aware entropy minimization loss further enhances the model's generalization to weakly and unlabeled regions. Experimental results demonstrate that our approach consistently outperforms existing fully supervised methods on both in-distribution and out-of-distribution data. Our work provides a new perspective for low-cost annotation and weakly supervised learning in IML, and significantly advances the development of this field.

REFERENCES

- [1] J. Dong, W. Wang, and T. Tan, "Casia image tampering detection evaluation database," in *2013 IEEE China summit and international conference on signal and information processing*. IEEE, 2013, pp. 422–426.
- [2] B. Wen, Y. Zhu, R. Subramanian, T.-T. Ng, X. Shen, and S. Winkler, "Coverage—a novel database for copy-move forgery detection," in *2016 IEEE international conference on image processing (ICIP)*. IEEE, 2016, pp. 161–165.
- [3] J. Hsu and S. Chang, "Columbia uncompressed image splicing detection evaluation dataset," *Columbia DVMM Research Lab*, vol. 6, 2006.
- [4] H. Guan, M. Kozak, E. Robertson, Y. Lee, A. N. Yates, A. Delgado, D. Zhou, T. Kheyrkhan, J. Smith, and J. Fiscus, "Mfc datasets: Large-scale benchmark datasets for media forensic challenge evaluation," in *2019 IEEE Winter Applications of Computer Vision Workshops (WACVW)*. IEEE, 2019, pp. 63–72.
- [5] F. Guilaro, D. Cozzolino, A. Sud, N. Dufour, and L. Verdoliva, "Trufor: Leveraging all-round clues for trustworthy image forgery detection and localization," in *Proceedings of the IEEE/CVF conference on computer vision and pattern recognition*, 2023, pp. 20 606–20 615.
- [6] Y. Chen, H. Cheng, H. Wang, X. Liu, F. Chen, F. Li, X. Zhang, and M. Wang, "Ean: Edge-aware network for image manipulation localization," *IEEE Transactions on Circuits and Systems for Video Technology*, 2024.
- [7] C. Kong, A. Luo, S. Wang, H. Li, A. Rocha, and A. C. Kot, "Pixel-inconsistency modeling for image manipulation localization," *IEEE Transactions on Pattern Analysis and Machine Intelligence*, pp. 1–18, 2025.
- [8] Y. Zhai, T. Luan, D. Doermann, and J. Yuan, "Towards generic image manipulation detection with weakly-supervised self-consistency learning," in *Proceedings of the IEEE/CVF International Conference on Computer Vision*, 2023, pp. 22 390–22 400.
- [9] Y. Zhou, H. Wang, Q. Zeng, R. Zhang, and S. Meng, "Exploring weakly-supervised image manipulation localization with tampering edge-based class activation map," *Expert Systems with Applications*, vol. 249, p. 123501, 2024. [Online]. Available: <https://www.sciencedirect.com/science/article/pii/S095741742400366X>
- [10] Z. Zhu, J. Li, and Y. Wen, "Self-optimization training for weakly supervised image manipulation localization," in *ICASSP 2025 - 2025 IEEE International Conference on Acoustics, Speech and Signal Processing (ICASSP)*, 2025, pp. 1–5.
- [11] R. Bai, "Weakly-supervised cross-contrastive learning network for image manipulation detection and localization," *Knowledge-Based Systems*, vol. 310, p. 113033, 2025.
- [12] W. Wang, E. Xie, X. Li, D.-P. Fan, K. Song, D. Liang, T. Lu, P. Luo, and L. Shao, "Pvt v2: Improved baselines with pyramid vision transformer," *Computational Visual Media*, vol. 8, no. 3, pp. 415–424, 2022.
- [13] R. He, Q. Dong, J. Lin, and R. W. Lau, "Weakly-supervised camouflaged object detection with scribble annotations," in *Proceedings of the AAAI conference on artificial intelligence*, vol. 37, no. 1, 2023, pp. 781–789.
- [14] A. Obukhov, S. Georgoulis, D. Dai, and L. Van Gool, "Gated crf loss for weakly supervised semantic image segmentation," *arXiv preprint arXiv:1906.04651*, 2019.
- [15] K. Roth, L. Pemula, J. Zepeda, B. Schölkopf, T. Brox, and P. Gehler, "Towards total recall in industrial anomaly detection," in *Proceedings of the IEEE/CVF conference on computer vision and pattern recognition*, 2022, pp. 14 318–14 328.
- [16] J. Zhu, Y. Guo, G. Sun, L. Yang, M. Deng, and J. Chen, "Unsupervised domain adaptation semantic segmentation of high-resolution remote sensing imagery with invariant domain-level prototype memory," *IEEE Transactions on Geoscience and Remote Sensing*, vol. 61, pp. 1–18, 2023.
- [17] A. Novozamsky, B. Mahdian, and S. Saic, "Imd2020: A large-scale annotated dataset tailored for detecting manipulated images," in *2020 IEEE Winter Applications of Computer Vision Workshops (WACVW)*, March 2020, pp. 71–80.
- [18] J. Nichol, P. Dhariwal, A. Ramesh, P. Shyam, P. Mishkin, B. McGrew, I. Sutskever, and M. Chen, "Glide: Towards photorealistic image generation and editing with text-guided diffusion models," *arXiv preprint arXiv:2112.10741*, 2021.
- [19] M. Huh, A. Liu, A. Owens, and A. A. Efros, "Fighting fake news: Image splice detection via learned self-consistency," in *Proceedings of the European conference on computer vision (ECCV)*, 2018, pp. 101–117.
- [20] T. J. De Carvalho, C. Riess, E. Angelopoulou, H. Pedrini, and A. de Rezende Rocha, "Exposing digital image forgeries by illumination color classification," *IEEE Transactions on Information Forensics and Security*, vol. 8, no. 7, pp. 1182–1194, 2013.
- [21] P. Korus and J. Huang, "Evaluation of random field models in multi-modal unsupervised tampering localization," in *2016 IEEE international workshop on information forensics and security (WIFS)*. IEEE, 2016, pp. 1–6.
- [22] X. Ma, X. Zhu, L. Su, B. Du, Z. Jiang, B. Tong, Z. Lei, X. Yang, C.-M. Pun, J. Lv *et al.*, "Imdl-benco: A comprehensive benchmark and codebase for image manipulation detection & localization," *Advances in Neural Information Processing Systems*, vol. 37, pp. 134 591–134 613, 2025.
- [23] X. Chen, C. Dong, J. Ji, j. Cao, and X. Li, "Image manipulation detection by multi-view multi-scale supervision," in *The IEEE International Conference on Computer Vision (ICCV)*, 2021.
- [24] X. Liu, Y. Liu, J. Chen, and X. Liu, "Psc-net: Progressive spatio-channel correlation network for image manipulation detection and localization," *IEEE Transactions on Circuits and Systems for Video Technology*, vol. 32, no. 11, pp. 7505–7517, 2022.
- [25] R. Ren, Q. Hao, S. Niu, K. Xiong, J. Zhang, and M. Wang, "Mfinet: Multi-feature fusion identification networks for artificial intelligence manipulation," *IEEE Transactions on Circuits and Systems for Video Technology*, vol. 34, no. 2, pp. 1266–1280, 2024.
- [26] L. Su, X. Ma, X. Zhu, C. Niu, Z. Lei, and J.-Z. Zhou, "Can we get rid of handcrafted feature extractors? sparsevit: Nonsemantics-centered, parameter-efficient image manipulation localization through spare-coding transformer," in *Proceedings of the AAAI Conference on Artificial Intelligence*, vol. 39, no. 7, 2025, pp. 7024–7032.
- [27] C. Kong, A. Luo, S. Wang, H. Li, A. Rocha, and A. C. Kot, "Pixel-inconsistency modeling for image manipulation localization," *IEEE Transactions on Pattern Analysis and Machine Intelligence*, 2025.
- [28] X. Zhu, X. Ma, L. Su, Z. Jiang, B. Du, X. Wang, Z. Lei, W. Feng, C.-M. Pun, and J.-Z. Zhou, "Mesoscopic insights: orchestrating multi-scale & hybrid architecture for image manipulation localization," in *Proceedings of the AAAI Conference on Artificial Intelligence*, vol. 39, no. 10, 2025, pp. 11 022–11 030.
- [29] C. Dong, X. Chen, R. Hu, J. Cao, and X. Li, "Mvss-net: Multi-view multi-scale supervised networks for image manipulation detection," *IEEE Transactions on Pattern Analysis and Machine Intelligence*, pp. 1–14, 2022.